Sensors & Transducers, Vol. 27, Special Issue, May 2014, pp. 29-38

Sensors & Transducers

Proteus Mirabilis Bacteria Biosensor Development Based on Modified Gold Electrode with 4-Carboxyphenyl Diazonium Salts for Heavy Metals Toxicity Detection

[1] Yosra BRAHAM, [1] Houcine BARHOUMI, [1] Abderrazak MAAREF, [2] Amina BAKHROUF and [3] Nicole JAFFREZIC-RENAULT

[1] Laboratory of Interfaces and Advanced Materials (LIMA), University of Monastir 5000, Tunisia
[2] Laboratory of analysis, treatment and valorization of environment pollutants and products, Faculty of Pharmacia, University of Monastir, 5000, Tunisia
[3] Laboratory of Analytical Sciences, UMR CNRS 5180, University of Claude Bernard-Lyon1, Bâtiment Raulin, 69622 Villeurbanne Cedex, France
[1] Tel.: + (216) 73 500 278, fax: + (216) 73 500 280
E-mail: Houcine.Barhoumi@fsm.rnu.tn

Received: 31 December 2012 /Accepted: 10 August 2013 /Published: 26 May 2014

Abstract: In this work we describe a new biosensor for heavy metals detection, based on the immobilization of bacteria, Proteus mirabilis on gold electrode modified with aryl electrografting film. To enhance the stability of the biosystem, additional materials were used such as functionalized Fe_3O_4 nanoparticles (NPs), cationic (PAH), anionic (PSS) polyelectrolytes, Bovine Serum Albumin (BSA) and glutaraldehyde as a cross-linking agent. Before the immobilization step, the activity of Proteus mirabilis bacteria in the presence of heavy metals ions was attempted using the ion ammonium selective electrodes (ISEs). The modification of the gold electrodes with the electrochemical reduction of 4-carboxyphenyl diazonium salts to form stable layers for sensing applications was characterized by cyclic voltammetry and chronoamperometry measurements. The adhesion of the bacteria cell on gold electrode was evaluated using contact angle measurements. The immobilized bacteria-metal interaction was evaluated using the electrochemical impedance spectroscopy (EIS) measurements. A notable effect of metal on the bacteria activity is observed in the concentration range from 10^{-3} to 1 µM and from 1µM to 1nM for Co^{2+}, Cd^{2+}, Cu^{2+} and Hg^{2+}, respectively.

Keywords: Proteus mirabilis bacteria, Fe_3O_4 nanoparticles, Diazonium salts, Impedance spectroscopy, Gold electrodes, Heavy metals.

1. Introduction

Heavy metals generally exert an inhibitory action on bacteria by either, blocking essential functional groups, displacing essential metal ions, or modifying the active conformations of biological molecules [1]. In naturally polluted environments, the response of microbial species to heavy metal ions depends on the concentration and availability of metals and is dependent on the actions of complex processes, controlled by multiple factors such as the type of metal (Hg, Co, Cd, Cu,) and the nature of the medium [2]. In fact, the great interest for applications in materials science, sensors and biology require the

development of efficient and stable biosensors to detect heavy metals at low concentration.

As known, biosensors based on nanoparticles [3, 4] and electrochemical grafted organic aryl film on gold surface [5], are attractive, simple, stable and powerful. However, nanoparticles involve one of the most interesting approaches to improve the electrochemical performances of the biosensor due to their large specific area and high surface free energy. The Fe_3O_4 nanoparticles have been considered as suitable for the immobilization of bacteria and enzyme due to the super paramagnetic behavior and the low toxicity [6-8].

Electrochemical biosensor possess a biomolecule as a reactive surface in close proximity to a transducer, which converts the binding of an analyte to the capturing biomolecule into a measurable signal [9], and have the advantage of being highly sensitive, rapid, and inexpensive [10]. The biosensor measure the change in electrical properties of electrode structures as cells become entrapped or immobilized on or near the electrode. In this work our study reports the modification of gold electrode with aryl film, magnetic nanoparticles and prokaryotic cells bacteria. The choice of this immobilization method offers a multitude to developing a new sensitive microorganism impedimetric biosensor for heavy metals detection. Moreover, 4-carboxyphenyl (4-CP) film was grafted by electrochemical reduction of in situ generated 4-carboxyphenyl diazonium salt (4-CPDS) in acidic aqueous solution without the isolation of the diazonium salt, followed by carbodiimide/succinimide (EDC/NHS). The electrochemical grafting process was evaluated by chronoamperometry and cyclic voltammetry. In addition, the deposit multi-layers on the gold electrode were evaluated using the electrochemical impedance spectroscopy technique. The performance of the developed biosensor in the presence of heavy metal ions was correlated with the interface's electrical properties based on the bacteria viability and its adherence to the substrate [11, 12].

2. Experiments

2.1. Reagents

The used bacteria were Proteus mirabilis (gram negative) diluted in PBS, provided by the laboratory of bacteria in Monastir. The concentration stability over time was controlled with OD (optical density) measurements. Sodium nitrite, 4-Aminobenzoic acid, Potassium ferricyanide ($K_3[Fe(CN)_6]$), potassium ferrocyanide ($K_4[Fe(CN)_6]$), sodium chloride (NaCl), potassium chloride (KCl), sodium phosphate (Na_2HPO_4), potassium phosphate (KH_2PO_4), sulfuric acid (98 %), hydrogen peroxide (30 %), N-hydroxysuccinimide (NHS), 1-ethyl-3-(3-dimethylaminopropyl)-carbodiimide hydrochloride (EDC), hydrochloride, glutaraldehyde, PAH (poly (allylamine hydrochloride), PSS (poly (sodium 4-styrene sulfonate), bovine serum albumin (BSA),glycerol and glutaraldehyde were purchased from Sigma–Aldrich. 2-(N-morpholino) ethanesulfonic acid (MES), was obtained from Sigma Chemicals. The iron oxide carboxyl-modified magnetic nanoparticles (MNPs, diameter = 200 nm, density of carboxyl groups > 350 μmol/g, stored in an aqueous suspension of 0.09 % NaN_3) were obtained from Ademtech. The heavy metals tested were sulfate salts: $CuSO_4.5H_20$, $HgSO_4$, $3CdSO_4.8H_20$ and, $COSO_4.7H_2O$. Phosphate buffer saline (PBS) adjusted at pH 7.4 containing 137 mM NaCl, 2.7 mM KCl, 10 mM Na_2HPO_4 and 1.8 mM KH_2PO_4 was used. A 5 mM of potassium ferricyanide/ferrocyanide solution prepared in PBS was used in EIS and CV experiments.

2.2. Gold Electrode Cleaning

Gold substrates were fabricated using standard silicon technologies. (100) oriented, P-type (3–5 Ω cm) silicon wafers were thermally oxidized to grow an 800 nm-thick field oxide. Then, a 30 nm thick titanium layer and a 300 nm thick gold layer were deposited by evaporation. They were provided by the Laboratory of Analyze and Architecture of Systems (LAAS), CNRS Toulouse. Before the modification step, the plate gold electrodes (1 cm × 1 cm) were cleaned in acetone solution for 20 min with ultrasonic bath. After that, they were dried under a nitrogen flow and then dipped for 1 min into a piranha solution of H_2SO_4/H_2O_2 (3:1 (v/v)). Finally, the gold substrates were vigorously rinsed with ultrapure water and immediately immersed in an ethanol solution and finally dried under a nitrogen flow.

2.3. Electrochemical Characterizations and Instrumentation

2.3.1. Potentiometric Measurements Based on Ion Selective Electrode (ISE)

Potentiometric method based on ion-selective electrodes (ISEs) offers advantages such as simple procedure, relatively fast response time, non-destructive analysis, wide linear range with moderate selectivity [13, 14] and extensively applied for the determination of many ions. In our work the potentiometric method was based on the measure of the potential or the ammonium ions concentration in the solution as function of the time when the proteus mirabilis urease interacts with urea. The potentiometic measurements were carried out using ammonium selective electrode and Ag/AgCl as reference electrode.

2.3.2. Electrochemical Impedance Spectroscopy Measurements

Electrochemical experiments were performed using a potentiostat–galvanostat (Voltalab-40) and the voltamaster 4 software with a conventional three-electrodes cell including a saturated calomel electrode (SCE) as the reference electrode, a platinum electrode (0.45 cm^2) as the counter electrode and the modified gold electrode (0.07 cm^2) as the working electrode. The impedance and cyclic voltammetry measurements were performed using the PBS as supporting electrolyte (pH=7.4) containing 5 mM of $Fe(CN)_6^{3-/4-}$ as the redox probe. The impedance spectra were recorded in a frequency range from 100 kHz to 100 mHz at the free potential of the used redox couple. The amplitude of the alternating voltage was 10 mV. All experiments were performed at 25 °C in a Faraday cage.

2.4. Contact Angle Measurements

It is generally agreed that the physicochemical properties of bacterial cell and substratum surfaces are the main factors mediating bacterial adhesion [15-17]. It is assumed that bacterial cell and substratum hydrophobicity is the key parameter controlling the non-specific interactions of the adhesion process [18]. Contact angle measurements with three different liquids (Water, formamide and diiodomethane) were performed with contact angle instrument ‘‘Digidrop’’ model from the society GBX (Romans, France). Every reported contact angle measurements represent an average value of at least three separated drops on different areas of the given wafer. The size and volume of the drops were kept constant since [19]. Furthermore, the surface energy components, the total energy (γ_s), the dispersive energy (γ^{LW}), the acid base energy:

$$\left(\gamma^{AB} = 2\sqrt{\gamma^+ \times \gamma^-}\right)$$

The acid energy (γ^+) and the basic energy (γ^-) were determined from the wetting angle according to the Van Oss equation with polar and apolar liquids [20].

2.5. Preparation of the Proteus Mirabilis Bacteria Biosensors

To ensure a high sensitivity and a good reproducible biosensor, various working conditions were taken account such as the presence of BSA and glycerol, the nanoparticles concentration (0.01 mg of NPs in 500 µL of PBS), the bacteria concentration (10^7 CFU/mL), the cross-linking time (30 min), the buffer solution concentration PBS (10 mM) and the number of the polyelectrolyte layers (n=3). In fact, the bacteria mixture was prepared by dissolving 5 mg of BSA in 100 µL of PBS bacteria solution, containing 10 µL of glycerol at pH 7.4. The initial NPs suspension (1/500) was sonicated for 15 min, then coated during 20 min, with an initial “preconditioning” layer of PAH (5 mg/mL) which provides a positive charge, followed by a layer of PSS (5 mg/mL) of opposite charge to form the first polyelectrolyte (PE) bilayer (n=1). The NPs were further coated sequentially with PEs, in the alternating order PAH/PSS until three bilayers, followed by a layer of PAH. We obtained (NPs-$(PAH\text{-}PSS)_n$/PAH) with n varies from 1 to 3. The PE rich supernatant phase was then eliminated and the NPs were rinsed twice with ultrapure water [21].

The clean Au electrode surface was dipped in the diazotation mixture, using instead (1:1 equiv) of $NaNO_2$ and 4-aminobenzoic acid [22], since an excess of nitrous acid exerts a very unfavorable influence on the stability of the diazotation solutions [23]. In general, 2 mM $NaNO_2$ solution was added to the electrolytic solution containing 2 mM of 4-aminobenzoic acid and 0.5 M HCl. The mixture was stirred and left to react for about 5 min at room temperature. The electrochemical reductive modification of gold with in situ generated 4-carboxyphenyl diazonium salt (4-CPDS) was carried out by cyclic voltammetry and chronoamperometric techniques. After modification, the 4-carboxyphenyl modified electrode (4-CP/Au) was rinsed thoroughly with copious amounts of water and used for the next step. The terminal carboxylic groups on gold electrode surface were activated by immersing the 4-CP/Au electrode in a stirred solution of 20 mM EDC and 4 mM NHS in 100 mM MES buffer (pH 6.8) for 60 min. After thorough rinsing with MES buffer, the modified electrode surface was covered with 10 µL of nanoparticles coated with $(PAH/PSS)_3$/PAH, then 10 µL of the bacteria mixture.

Finally, the 4-CP/NPs-$(PAH\text{-}PSS)_3$/PAH-Proteus mirabilis/Au modified electrode, (Fig. 1) was kept in Glutaraldehyde vapor for 30 min to allow the reticulation of the bacteria. After incubation, the electrode was rinsed with water to remove unbounded bacteria. The modified electrode can then be used for electrochemical measurements or should be stored at 4 °C. For the inhibition study in homogeneous phase, 1.16 mM of each metal such as Hg, Co, Cd, and Cu was prepared in PBS to be used as test solution to incubate bacteria during 30 min.

3. Results and Discussion

3.1. Study of the Heavy Metal-Bacteria Interaction in Homogeneous Phase

The characterization principle was based on the fact that urease from Proteus mirabilis catalyzes the hydrolysis of the transformation of urea

into carbon dioxide and ammonium [24], according to the following reaction:

$$CO(NH_2)_2 + 3\,H_2O \xrightarrow{Urease} 2NH_4^+ + HCO_3^- + OH^- \quad (1)$$

The effect of heavy metals incubated with 12 mL of the bacteria solution for 30 minutes was evaluated by using the potentiometric method based on the reference and the ammonium ion-selective electrodes.

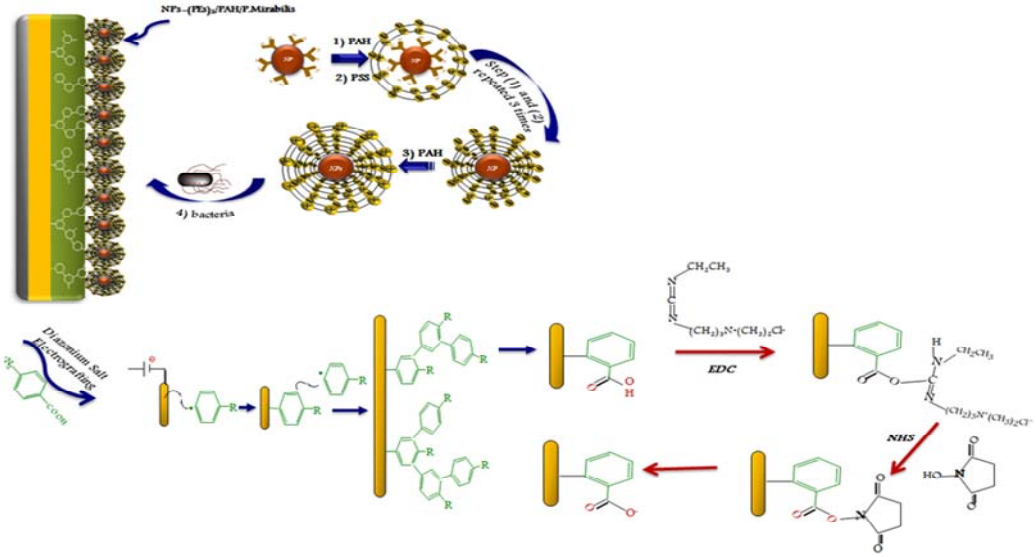

Fig. 1. Schematic of the biosensor elaboration using 4-CP and Fe_3O_4 nanoparticles.

Fig. 2 shows a Michaelien behaviour defined by the variation of the ammonium ion concentration as function of the time for different tested metal ions at fixed concentration of 1.16 mM and in the presence of 1.4 mM of urea.

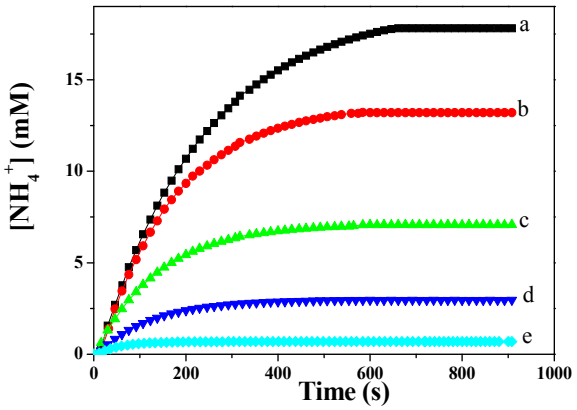

Fig. 2. Kinetic behaviour of the enzymatic reaction according to the metal effect on the free bacteria without (a) and with 1.16 mM of Cu^{2+} (b), Cd^{2+} (c), Co^{2+} (d) , Hg^{2+} (e) heavy metal ions.

This figure demonstrates the high inhibitor effect of the Hg ions compared to the other tested heavy metal ions. As result, the inhibitor behaviour was characterized by the following order of toxicity

Hg > Co > Cd > Cu.

Table 1 presents the activity of bacteria, the ammonium quantity and the inhibition rate due to the metals ions effect.

Table 1. Variation of the ammonium amount, the activity and the inhibition rate for the free bacteria incubated without and with the heavy metal ions.

	NH_4^+ (µmol)	Activity (µmol/min)	Inhibition (%)
Bacteria	213.6	19.4	0
Bacteria/Cu^{2+}	158.4	15.8	25
Bacteria/Cd^{2+}	84.0	8.6	60
Bacteria/Co^{2+}	34.8	3.6	83
Bacteria/Hg^{2+}	7.2	1.4	96

These parameters were calculated for the free bacteria before and after the incubation process with the heavy metal ions. The inhibition rate was calculated based on the following relation:

$$Inhibition(\%) = \frac{C_0 - C_i}{C_0} \times 100 \quad (2)$$

With C_0 and C_i correspond to the NH_4^+ concentration generated by the free bacteria before and after the incubation step with the heavy metal ions.

It appears that a rate of appreciable inhibition was observed for Hg^{2+} that corresponds to a significant percentage equal to 96 % and remains less important for the other tested heavy metal ions.

3.2. Study of the Heavy Metal Iions Effect on the Immobilized Bacteria

3.2.1. Modified Gold Electrode with Aryl Diazonium Salt

Fig. 3a shows the voltammogram of the Au modified electrode with the 4-carboxyphenyl diazonium salt in situ from 0.4 to -0.4 V at 100 mVs^{-1}. An irreversible cathodic peak was observed at -0.1 V/SCE attributed to the reduction of the diazonium species via one electron process leading to 4-CP radicals that bind to the gold surface. An irreversible formation of a strongly bonded organic layer to the surface can be obtained with no associated oxidation peak indicative of the loss of N_2 groups. The very low cathodic reduction potential is characteristic of the diazonium salts [25]. The surface coverage Γ was estimated from the integration of the charge passed Q under the voltammetric peaks reaches 1.6610^{-8} mol cm^{-2} of molecules grafted to the surface.

$$\Gamma = \frac{Q}{nFS}, \qquad (3)$$

where n is the electrons number consumed per grafted molecule, F the Faraday constant (F= 96500 $C.mol^{-1}$) and S is the geometric surface of the electrode (0.07 cm^2).

The number of electrons transferred is higher than that observed for the theoretical maximum surface coverage for a diazonium salt derived monolayer of 12×10^{-10} mol cm^{-2} [26].

This estimated higher value was in good agreement with the value discussed by Belanger and co-workers (12.2×10^{-10} mol cm^{-2}) [27]. To avoid multilayers formation of the grafted 4-CP we have used the chronoamperometry (CA) method (Fig. 3b).This technique can leads to an ordered monolayer with uniform density in which all terminal carboxylic groups remain accessible to react with the attached poly-electrolytes and then to the immobilized bacteria.

When the gold electrode was modified with the 4-carboxyphenyl monolayer the quantity of electrons generated during the experiment can be calculated from the charge Q delivered over time which is equivalent to the integral of the i(t) curve. It is easy to evaluate the number of the moles of electrons n since Q = n.N_A.e (with N_A the Avogadro's number, e the elementary charge carried by an electron and N_A.e = F the Faraday constant). For Q = -20 10^{-6} C, the system produces 2×10^{-10} moles of electrons. The surface coverage, Γ estimated from CA is equal to 3 10^{-9} mol.cm^{-2} of molecules attached to the surface was relative to the electrons transferred to the diazonium salts.

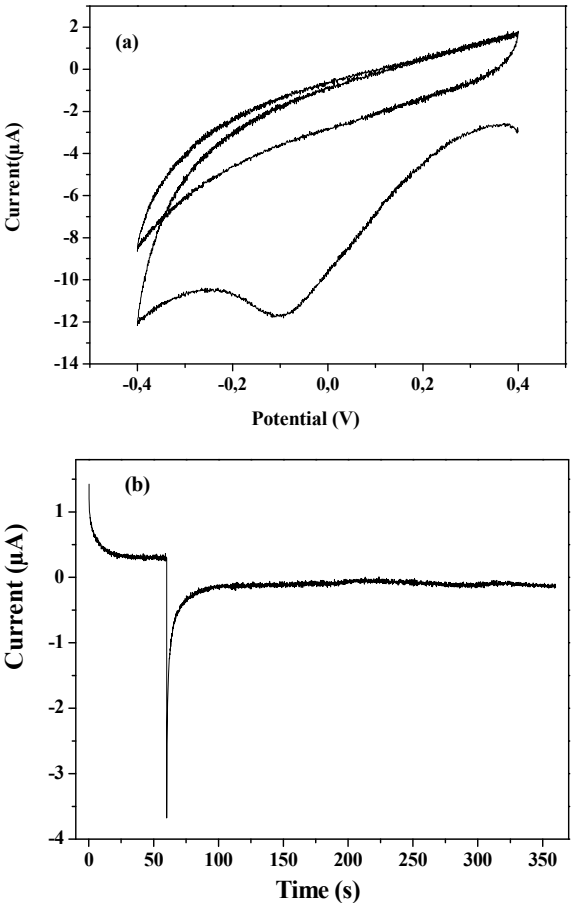

Fig. 3. Cyclic voltammogram, at scan rate of 100 mVs^{-1} (a) and Chronoamperometric curve, at applied potential of -0.4 V/SCE for 5 min (b), for the in situ generated 4-carboxyphenyl diazonium salt (4-CPDS) in the diazotation mixture (2 mM $NaNO_2$ + 2 mM 4-aminobenzoic acid in 0.5 HCl) at Au electrode in 0.5 M HCl.

3.2.2. Proteus Mirabilis Biosensor Characterizations

The cyclic voltammogram of soluble electroactive species provides a convenient tool to monitor the various stages of the biosensor buildup on Au electrode.

Fig. 4 (a) shows the voltammograms of 5 mM $[Fe(CN)_6]^{4-/3-}$ probe for the bare and the modified Au electrodes in PBS, pH 7.4, at scan rate of 100 mVs^{-1}. The Au surface was modified with different layers such as

4-CP, NPs-$(PAH\text{-}PSS)_3$/PAH-Proteus/mirabilis or

4-CP/NPs-$(PAH\text{-}PSS)_3$/PAH-Proteus mirabilis.

It can be seen that for a bare Au electrode, a characteristic quasi-reversible redox cycle with anodic and cathodic peak currents were

obtained. When the Au surface was functionalized with the 4-CP layer the electron transfer between the redox probe and the modified surface was severely blocked. As a result, an obvious disappearance of the anodic and the cathodic peaks was observed leading to a high ΔEp value (340 mV) indicating the formation of the CP layer.

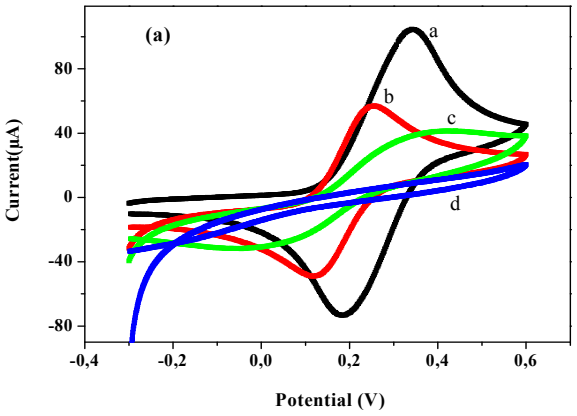

(a)

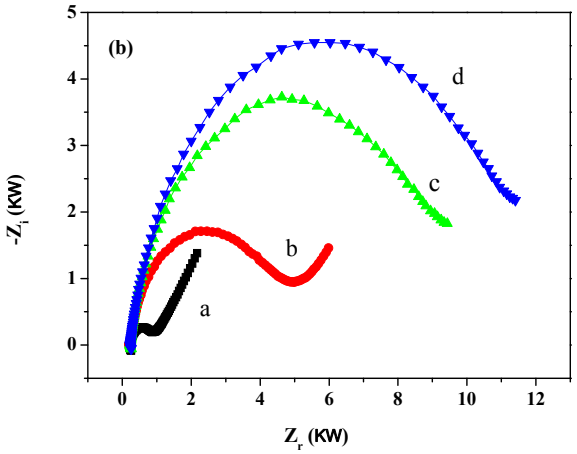

(b)

Fig. 4. Cyclic voltammograms (a) and the Nyquist plots (b) using a frequency range of 100 kHz to 100 MHz for the bare Au (1); NPs-(PAH-PSS)$_3$/PAH-Proteus mirabilis/Au (2); 4-CP/NPs-(PAH-PSS)$_3$/PAH-Proteus mirabilis/Au (3) and 4-CP/Au (4) modified electrodes.

Electrochemical impedance spectroscopy can also gives detailed information on the dielectric constant and the barrier properties of the deposit layer changes. Fig. 4b, shows the impedance spectra of the bare and the modified gold electrode. The bare Au electrode reveals a very small semicircle, implying a very low electron-transfer resistance (R_{et}) of the redox probe. When the electrode is grafted with the 4-CP film, the R_{et} increases significantly. The deposit film was defined with negatively charged (COO^-) which acts as an electrostatic barrier that resists to the $[Fe(CN)_6]^{4-/3-}$ redox probe and hinder its ability to diffuse into the layer. As a result, this phenomenon retards the electron transfer kinetics between the redox probe and the modified electrode. Subsequently, nanoparticles coated with PAH polyelectrolytes positively charged were deposited onto the 4-CP modified electrode and a remarkable decrease in the R_{et} was observed. It is likely that the electrostatic attachment of the PAH to the carboxyl terminus will neutralize the negative charge of 4-CP modified electrode. We note, that the electrochemistry of the NPs-(PAH-PSS)$_3$/PAH-Proteus mirabilis/Au modified electrode surface is still observable, indicating that the polyelectrolyte layers does not provide a very effective barrier between the electrolyte and the gold surface. The change in the charge transfer resistance is related to the electrode coverage τ and is given by the relation as shown in the following relation:

$$\tau(\%) = \frac{R_{et} - R_{et}^0}{R_{et}} \times 100, \qquad (4)$$

where τ is the apparent electrode coverage, R_{et}° and R_{et} are the electron transfer resistance measured at the bare and the modified Au electrode, respectively. The coverage rates (τ) of the modified electrode were reported in Table. 2. As result, a higher coverage rate was observed for 4-CP/Au and 4-CP/NPs-(PAH-PSS)$_3$/PAH-Proteus mirabilis/Au electrodes in comparison with the NPs-(PAH-PSS)$_3$/PAH-Proteus mirabilis/Au electrode. This behaviour proves the effectiveness of the procedure modification since the diazonium molecules cover the quasi-totality of the electrode surface. These results are in good agreement with those reported in a previous work [28].

Table 2. Impedance parameters of the deposited layers on gold electrode obtained by experimental fitting data to the equivalent circuit model in Fig. 5. for the bare Au (1); CP/Au (2);NPs-(PAH-PSS)$_3$/PAH-Proteus mirabilis/Au (3) and 4-CP/NPs-(PAH-PSS)$_3$/PAH-Proteus mirabilis/Au (4).

	ΔEp (mV)	Rs (Ω)	C_{dl} (μF)	R_{et} (Ω)	X^2 (10^{-3})	τ (%)
(1)	150	210	7.22	763	1.46	0
(2)	340	230	4.10	11502	1.46	93
(3)	125	226	6.77	5352	3.20	85
(4)	337	227	5.51	9408	1.10	92

The impedance data were fitted to a simple Randles equivalent circuit presented in the Fig. 5 which was made up of a parallel combination of the solution resistance (R_s), the electron transfer resistance (R_{et}), the constant phase element (C_{dl}) and the warburg impedance element (W). Thus, R_{et} was a suitable signal for sensing the interfacial properties of the prepared biosensor during the assembly procedure.

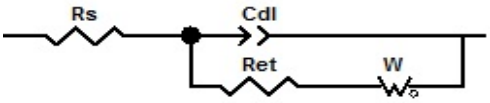

Fig. 5. The equivalent circuit model applied to simulate the impedance spectroscopy data.

3.2.3. Contact Angle Measurements and Adhesion Tests

Contact angle can be used as powerful technique to check the effectiveness of the functionnalization process. In our work we have used three liquids with different polarity (water, formamide and diiodomethane) for hydrophilic/hydrophobic character and surface energy determination. In fact, the contact angle measurements obtained with different test liquids, were carried out on the bare and the modified gold electrode. The wetting properties have been compared before and after the functionnalization process. The contact angle values and the surface energy components are summarized in the Table 3. The contact angle error is about ± 3°.

The contact angle measurements show that the hydrophobic Au surface acquires a hydrophilic character when it is functionalized with the proteus mirabilis bacteria. As result, an increase in the basic energy (γ^-) of the modified surface was observed due to the hydroxide (OH) and the carboxyl (COOH) groups localized in proteus mirabilis bacteria and nanoparticles [29]. Table 4 presents the contact angles with the different probe liquids for Proteus mirabilis suspended in PBS and deposited on cellulose acetate membrane filters. With an angle of 18.1° we conclude that the bacterial cell presents a hydrophilic character. In adhesion phenomenon the contribution of the electrostatic forces is important, since together bacteria and 4-CP/Au surface have generally negative surface potentials, giving rise to repulsive electrostatic interactions. But, the use of the polyelectrolyte PAH reduces the repulsion effect and enhances the adhesion under through the positive charge of NH_3^+ cationic groups.

Table 3. Contact angles and surface energy components the bare and the modified Au electrode.

Contact angle (°)					Surface energy components (mJ/m²)			
Surface	**Water**	**Surface**	**Water**	**Surface**	**Water**	**Surface**	**Water**	**Surface**
Bare Au	71.7	Bare Au	71.7	Bare Au	71.7	Bare Au	71.7	Bare Au
Au/4-CP	67.7	Au/4-CP	67.7	Au/4-CP	67.7	Au/4-CP	67.7	Au/4-CP
Au /NPs-(PAH-PSS)$_3$/PAH	93.0	Au /NPs-(PAH-PSS)$_3$/PAH	93.0	Au /NPs-(PAH-PSS)$_3$/PAH	93.0	Au /NPs-(PAH-PSS)$_3$/PAH	93.0	Au /NPs-(PAH-PSS)$_3$/PAH
Au/ 4-CP/NPs-(PAH - PSS)$_3$/PAH	78.0	Au/ 4-CP/NPs-(PAH - PSS)$_3$/PAH	78.0	Au/ 4-CP/NPs-(PAH - PSS)$_3$/PAH	78.0	Au/ 4-CP/NPs-(PAH - PSS)$_3$/PAH	78.0	Au/ 4-CP/NPs-(PAH - PSS)$_3$/PAH
Au /4-CP/NPs-(PAH-PSS)$_3$/PAH-Proteus mirabilis	39.6	Au /4-CP/NPs-(PAH-PSS)$_3$/PAH-Proteus mirabilis	39.6	Au /4-CP/NPs-(PAH-PSS)$_3$/PAH-Proteus mirabilis	39.6	Au /4-CP/NPs-(PAH-PSS)$_3$/PAH-Proteus mirabilis	39.6	Au /4-CP/NPs-(PAH-PSS)$_3$/PAH-Proteus mirabilis
Au/ NPs-(PAH-PSS)$_3$/PAH-Proteus mirabilis	39.1	Au/ NPs-(PAH-PSS)$_3$/PAH-Proteus mirabilis	39.1	Au/ NPs-(PAH-PSS)$_3$/PAH-Proteus mirabilis	39.1	Au/ NPs-(PAH-PSS)$_3$/PAH-Proteus mirabilis	39.1	Au/ NPs-(PAH-PSS)$_3$/PAH-Proteus mirabilis

Table 4. Surface energy components of Proteus mirabilis suspended in PBS.

Surface energy components (mJ/m²)					
	γ^{LW}	γ^{AB}	γ^+	γ^-	γ^{Total}
Proteus mirabilis	37.6	15.8	1.3	55.6	53.5
PBS[b]	22.0	35.2	17.6	17.6	57.2

Using the thermodynamic approach of the Lifshitz van der Waals (LW) and acid/base (AB) interactions, the total adhesion energy ΔG_{adh}^{Total} of a bacterium to a substratum surface in a suspending liquid can be calculated as the sum of the LW component ΔG_{adh}^{LW} and the AB component ΔG_{adh}^{AB} [30-32].

$$\Delta G_{adh}^{Total} = \Delta G_{adh}^{LW} + \Delta G_{adh}^{AB} \quad (6)$$

$$\Delta G_{adh}^{LW} = (\sqrt{\gamma_B^{LW}} - \sqrt{\gamma_S^{LW}})^2 - (\sqrt{\gamma_B^{LW}} - \sqrt{\gamma_L^{LW}})^2 - \\ -(\sqrt{\gamma_S^{LW}} - \sqrt{\gamma_L^{LW}})^2 \quad (7)$$

$$\Delta G_{adh}^{LW} = 2[\sqrt{\gamma_L^+}(\sqrt{\gamma_B^-} + \sqrt{\gamma_S^-} - \sqrt{\gamma_L^-}) + \\ + \sqrt{\gamma_L^-}(\sqrt{\gamma_B^+} + \sqrt{\gamma_S^+} - \sqrt{\gamma_L^+}) - \sqrt{\gamma_B^-\gamma_S^+} - \sqrt{\gamma_B^+\gamma_S^-}] \quad (8)$$

The prediction of the thermodynamic approach states that adhesion may occur if ΔG_{adh}^{Total} is negative and it is energetically unfavorable if ΔG_{adh}^{Total} is positive. Using Equations (6), (7) and (8), the values of the interfacial free energy of adhesion of Proteus mirabils to the gold electrodes and its components (LW and AB) are calculated and presented in Table 5.

Table 5. Lifshitz van der Waals (ΔG_{adh}^{LW}), acid/base (ΔG_{adh}^{AB}) and total (ΔG_{adh}^{Total}) interfacial free energy of adhesion of Proteus mirabilis on Au surfaces (in millijoules per square meter).

Materials	ΔG_{adh}^{LW} (mJ/m^2)	ΔG_{adh}^{AB} (mJ/m^2)	ΔG_{adh}^{totale} (mJ/m^2)
Au	-5.55	2.72	-2.83
Au/ 4-CP	-5.16	8.88	3.72
Au/NPs-(PAH-PSS)$_3$/PAH	-4.73	-6.46	-11.19
Au/4-CP / NPs-(PAH-PSS)$_3$/PAH	-4.75	-7.72	-12.47

According to the thermodynamic approach, the negative value of the estimated energy demonstrates that the adhesion is favorable (Table 5). In fact, the adhesion process is governed by the electrostatic interactions. As result, the negative value of the LW adhesion energy component indicates that the adhesion was favorable onto the NPs-(PAH-PSS)$_3$/PAH and 4-CP/NPs-(PAH-PSS)$_3$/PAH modified Au surfaces with estimated total adhesion energy values of -11.19 and -12.47 mJ/m^2 respectively. This high adhesion energy indicates that Proteus mirabilis bacteria adhere strongly to the hydrophobic Au surface.

3.2.4. Impedance Study of the Immobilized Bacteria Inhibition by the Metal Ions

To evaluate the interaction between bacteria and the heavy metal ions the modified Au/4-CP/NPs-(PAH-PSS)$_3$/PAH-Proteus mirabilis electrode was incubated for 30 min in various heavy metal solutions for different concentrations such as Co, Cd, Cu and Hg ions. The recorded sensor output signal correlates directly with the respective metal concentrations in the PBS solution by the electrochemical impedance spectroscopy (EIS) measurement in a frequency range from 100 kHz to 100 mHz at the free potential.

It was found that the diameter of the semi circle decreases when the heavy metal ion concentration increases as can be seen in Fig. 6.

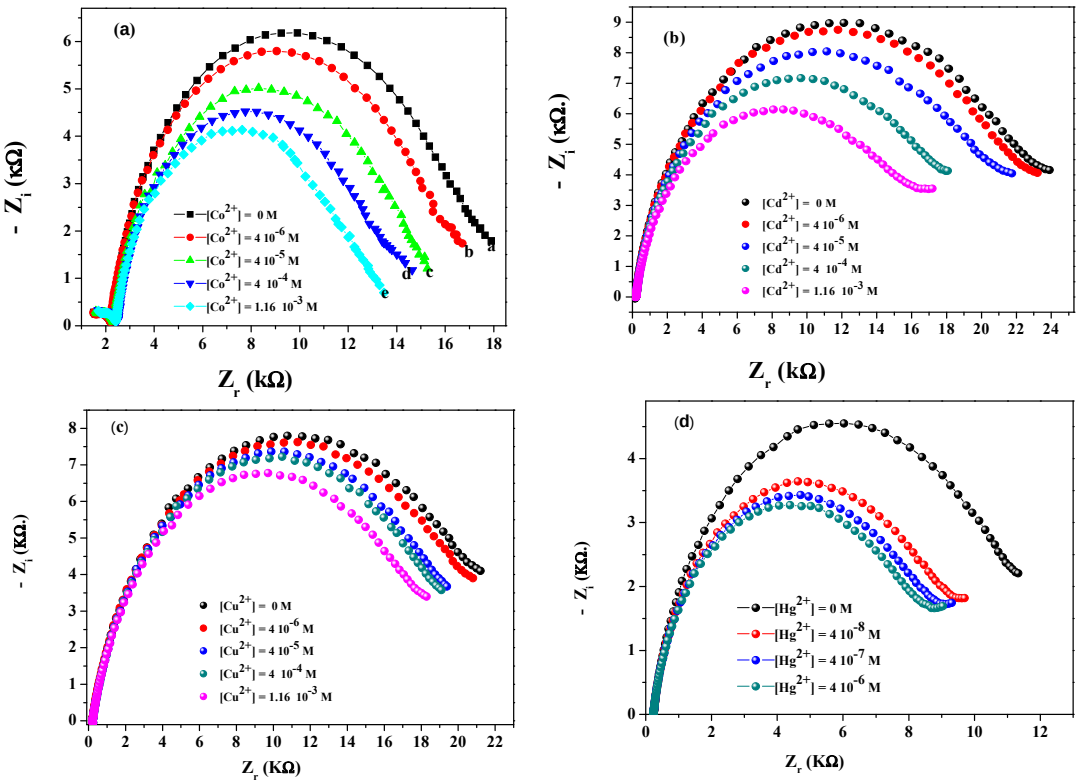

Fig. 6. Nyquist plots of electrochemical impedance spectra of Au/4-CP/NPs-(PAH-PSS)$_3$/PAH-Proteus mirabilis electrode for Co^{2+} (a), Cd^{2+} (b), Cu^{2+} (c) and Hg^{2+} ions (d).

Furthermore, to confirm the stability of the biosensor signal in the presence of the heavy metal ions, many tests were carried out on different modified electrodes prepared in the same conditions. We obtain a relative standard deviation of 4 % that proves the reproducibility of the developed biosensor. Among the tested heavy metal ions we note that the Au modified electrode presents a low detection limit for Hg^{2+} ions with a linear concentration range from 10^{-6}M to 10^{-9}M. This result confirms the high effect of the mercuric ions on the bacteria activity. In literature many studies have been reported describing the inhibition effect of heavy metal ions on the urease activity [24]. Among them it was demonstrated that mercury ion is the major inhibitor that presents a high affinity towards urease leading to a complete loss of its activity. In our work, we have used the Proteus mirabilis bacteria as an optimized medium to prevent urease from denaturation. In spite of the bacterium presence we conclude that the metal ion can diffuse through its membrane and bonds to urease. But, we signal here that heavy metal effect is less important in comparison with the inhibition of the free urease. Moreover, the Proteus mirabils biosensor presents a significant sensitivity towards Co^{2+} , Cd^{2+} and Cu^{2+} with a detection limit of 4 10^{-6}M and a linear concentration range from 10^{-3} to 4×10^{-6}M (Fig. 7).

Based on the numeric simulation data, the biosensor calibration curve presents a linear relation between R_{et} and the logarithm of the metal concentration (C). Indeed the R_{et} decreases when the concentration of the tested metal ions increases.

This effect can be attributed to the accumulation of the metal ions on the bacterium membrane leading to a conductive layer.

Also, the obtained results demonstrated that the heavy metal ions were found to inhibit free and immobilized urease in the following decreasing order:

Hg > Co > Cd > Cu

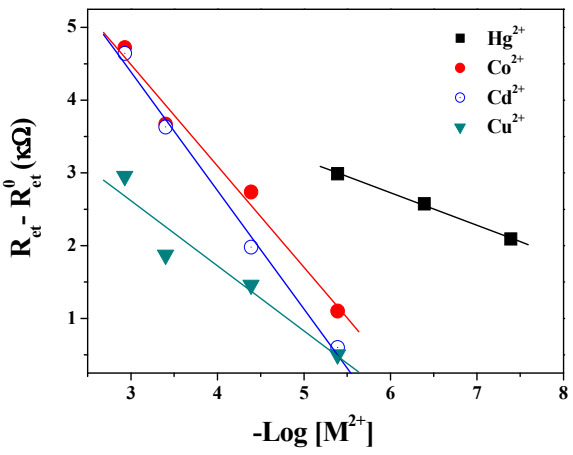

Fig. 7. Calibration curves of Au/4-CP/NPs-(PAH-PSS)$_3$/PAH-Proteus mirabilis biosensor describing the variation of the electron transfer resistance as function of the logarithm of the heavy metal ions concentration.

4. Conclusion

In this work, a renewable inhibitive heavy metal sensor is proposed based on self-assembling magnetic nanoparticles on a gold electrode. Firstly, magnetic nanoparticles were assembled on the surface of the electrografting 4-carboxyphenyl diazonium membrane. Then, bacteria were immobilized on the magnetic nanoparticles through physical adsorption using PAH and PSS plyelectrolytes. During the elaboration of the multi-layers system the deposit of such layer was evaluate by using electrochemical and wettability measurements. The developed bacteria biosensor was applied for heavy metal ions inhibition. Despite the presence of bacteria as optimized environment for urease we note a significant inhibition effect produced by some tested heavy metal ions. As result, immobilized Proteus mirabilis may be utilized as a bioindicator of the trace levels of these heavy metal ions in environmental monitoring, bioprocess and food control or pharmaceutical analysis.

Acknowledgements

The authors would like to thank CAMPUS-FRANCE for its support through PHC Maghreb No 12MAG088.

References

[1]. P. Doelman, E. Jansen, M. Michels, M. Van Til, Effects of heavy metals in soil on microbial diversity and activity as shown by the sensitivity-resistance index, an ecological relevant parameter, *Biology and Fertility of Soils*, Vol. 17, 1994, pp. 177-184.

[2]. A. Goblenz, K. Wolf, P. Bauda, The role of glutathione biosynthesis in heavy metal resistance in the fission yeast Schizosaccharomyces pompe. Metals and microorganisms: relationships and applications, *FEMS Microbiol. Rev*, Vol. 14, 1994, pp. 303-308.

[3]. Q. Pankhurst, J. Connolly, S. Jones, J. Dobson, Applications of magnetic nanoparticles in biomedicine, *Journal of Physics D Applied Physics*, Vol. 36, 2003, pp. 167-181.

[4]. P. V. Kamat, Photophysical, photochemical and photocatalytic aspects of metal nanoparticles, *Journal of Physical Chemistry B*, Vol. 106, 32, 2002, pp. 7729–7744.

[5]. J. Pinson, F. Podvorica, Attachment of organic layers to conductive or semiconductive surfaces by reduction of diazonium salts, *Chem. Soc. Rev*, Vol. 34, 2005, pp. 429–439.

[6]. R. Maalouf ,W. M. Hassen, C. Fournier-Wirth, N. Jaffrezic-Renault, Comparison of functionalized beads based on biosensor for bacteria detection to the self-assembled multilayer system, *Microchimica Acta*, Vol. 163, 2008, pp. 157-163.

[7]. A. K. Gupta, M. Gupta, Synthesis and surface engineering of iron oxide nanoparticles for

biomedical applications, *Biomaterials*, Vol. 26, 2005, pp. 3995-4021.

[8]. F. Y. Cheng, C. H. Su, Y. S. Yang, C. S. Yeh, C. Y. Tsai, C. L. Wu, M. T. Wu, D. B. Shi, Characterization of aqueous dispersions of Fe_3O_4 nanoparticles and their biomedical applications, *Biomaterials*, Vol. 26, 2005, pp. 729-738.

[9]. A. P. F Turner, I. Karurbe, G. S. Wilson, Eds., Biosensors, Fundamentals and Applications, *Oxford University Press*, Oxford, 1987.

[10]. A. Ghindilis, P. Atanasov, M. Wilkins, E. Wilkins, Immunosensors electrochemical sensing and other engineering approaches, *Biosens. Bioelectron*, Vol. 13, 1998, pp. 113-131.

[11]. I. Giaever, C. R. Keese, Use of electric fields to monitor the dynamical aspect of cell behavior in tissue culture, *IEEE Trans. Biomed.*, Vol. 33, 1986, pp. 242-247.

[12]. M. I. Prodromidis, Impedimetric immunosensors, *Electrochimica Acta*, Vol. 55, 2010, pp. 4227-4233.

[13]. M. Ghaedi, M. Montazerozohori, A. Mousavi, S. Khodadoust, M. Mansouri, Construction of new iodide selective electrodes based on bis(trans-cinnamaldehyde)1,3-propanediimine(L) zinc(II) chloride [ZnLCl2] and bis(trans-cinnamaldehyde) 1,3-propanediimine(L) cadmium(II) chloride [CdLCl2], *Materials Science and Engineering C*, Vol. 32, 2012, pp. 523-529.

[14]. M. Ghaedi, S. Naderi, M. Montazerozohori, R. Sahraei, A. Daneshfar, N. Taghavimoghadam, Modified carbon paste electrodes for Cu(II) determination, *Materials Science and Engineering C*, Vol. 32, 2012, pp. 2274-2279.

[15]. M. N. Bellon-Fontaine, N. Mozes, H. C. Van der Mei, J. Sjollema, O. Cerf, P. G. Rouxhet, H. J. Busscher, A comparison of thermodynamic approaches to predict the adhesion of dairy microorganisms to solid substrata, *Cell Biophysics*, Vol. 17, 1990, pp. 93-106.

[16]. A. M. Gallardo-Moreno, M. L. González-Martín, C. Pérez-Giraldo, J. M. Bruque, A. C. Gómez-García, Serum as a factor influencing adhesion of Enterococcus faecalis to glass and silicone, *Applied and Environmental Microbiology*, Vol. 68, 2002, pp. 5784-5787.

[17]. J. Wang, N. Huang, C. J. Pan, S. C. H. Kwok, P. Yang, Y. X. Leng, J. Y. Chen, H. Sun, G. J. Wan, Z. Y. Liu, P. K. Chu, Bacterial repellence from polyethylene terephthalate surface modified by acetylene plasma immersion ion implantation-deposition, *Surface Coatings Technology*, Vol. 186, 2004, pp. 299-304.

[18]. S. Bayoudh, A. Othmane, F. Bettaieb, A. Bakhrouf, H. Ben Ouada, L. Ponsonnet, Quantification of the adhesion free energy between bacteria and hydrophobic and hydrophilic substrata, *Materials Science and Engineering C*, Vol. 26, 2006, pp. 300 -305.

[19]. A. Marmur, Thermodynamic aspects of contact angle hysteresis, *Adv. Colloid Interface Sci*, Vol. 50, 1994, pp. 121-141.

[20]. C. J. Van Oss, R. J. Good, M. K. Chaudhurg, *J. Colloid Interface Sci*, Vol. 28, 1987, pp. 35-64.

[21]. S. Ciurli, S. Mangani., Nickel-containing enzymes, in: I. Bertini, A. Sigel, H. Sigel (Eds.), *Handbook on Metalloproteins*, Marcel Dekker, New York, 2001, pp. 669.

[22]. S. Baranton, D. Belanger, The use of aryl diazonium salts in the fabrication of biosensors and chemical sensors, *Journal of Physical Chemistry B*, Vol. 109, 2005, pp. 24401-24410.

[23]. H. Zollinger, Diazo, Aromatic and Heteroaromatic Compounds, *Chemistry I, VCH Publishers*, New York, 1994.

[24]. Grace Mary Ederer, Jackie H. Chu, and Donna J. Blazevic, Rapid Test for Urease and Phenylalanine Deaminase Production, *Appl. Microbiology*, Vol. 21, 1971, pp. 545.

[25]. P. Allongue, M. Delamar, B. Desbat, O. Fagebaume, R. Hitmi, J. Pinson, J. M. Saveant, Covalent Modification *of* Carbon Surfaces by Aryl Radicals Generated from the Electrochemical Reduction *of* Diazonium Salts, *Journal of Physical Chemistry Soc*, Vol. 119, 1997, pp. 201-207.

[26]. Y. C. Liu, R. L. McCreery, Reactions of organic monolayers on carbon surfaces observed with unenhanced Raman spectroscopy, *Journal of Physical Chemistry Soc*, Vol. 117, 1995, pp. 11254-11259.

[27]. A. Laforgue, T. Addou, D. Belanger, Characterization of the Deposition of Organic Molecules at the Surface of Gold by the Electrochemical reduction of Aryldiazonium Cations, *Langmuir*, Vol. 21, 2005, pp. 6855-6865.

[28]. J. Lu, X. He, X. Zeng, Q. Wan, Z. Zhang, Voltammetric determination of mercury (II) in aqueous media using glassy carbon electrodes modified with novel calix[4]arene, *Talanta*, Vol. 59, 2003, pp. 553-560.

[29]. E. Laviron, Interfacial Electrochem, *J. Electroanal. Chem* Vol. 10, 1979, pp. 19-28.

[30]. N. J. Hallab, K. J. Bundy, K. O. Connor, R. L. Moses, J. J. Jacobs, Evaluation of metallic and polymeric biomaterial surface energy and surface roughness characteristics for directed cell adhesion, *Tissue Engineering*, Vol. 7, 2001, pp. 55-71.

[31]. M. N. Bellon - Fontaine, N. Mozes, H. C. van der Mei, J. Sjollema, O. Cerf, P.G. Rouxhet, H. J. Busscher, A comparison of thermodynamic approaches to predict the adhesion of dairy microorganisms to solid substrata, *Cell Biophysics*, Vol. 17, 1990, pp. 93-106.

[32]. Van .Oss, C. J, Hydrophobicity of biosurfaces origin, quantitative determination and interaction energies, *Colloids Surfaces B,* Vol. 5, 1990, pp. 91-110.

[33]. T. Duxbury, Toxicity of heavy metals to soil bacteria, *FEMS Microbiol. Lett*, Vol. 11, 1981, pp. 217-220.
